The EMBO Journal Vol.18 No.21 pp.5931–5942, 1999

Intestinal polyposis in mice with a dominant stable mutation of the β-catenin gene

Naomoto Harada, Yoshitaka Tamai, Tomo-o Ishikawa, Brian Sauer[1,2], Kazuaki Takaku[3], Masanobu Oshima and Makoto M.Taketo[3,4]

Banyu Tsukuba Research Institute (Merck), Tsukuba 300-2611, [3]Laboratory of Biomedical Genetics, Graduate School of Pharmaceutical Sciences, The University of Tokyo, 7-3-1 Hongo, Bunkyo-ku, Tokyo 113-0033, Japan and [1]National Institute of Diabetes and Digestive and Kidney Diseases, National Institutes of Health, Bethesda, MD 20892-1800, USA

[2]Present address: Developmental Biology Program, Oklahoma Medical Research Foundation, Oklahoma City, OK 73104, USA

[4]Corresponding author
e-mail: taketo@mol.f.u-tokyo.ac.jp

Ectopic expression of certain *Wnt* genes in mouse mammary tissue is tumorigenic, and mutations that stabilize β-catenin are found in various human cancers including colorectal cancer. To determine the role of stabilized β-catenin in intestinal tumorigenesis in mice, we constructed by embryonic stem (ES) cell-mediated homologous recombination, a mutant β-catenin allele whose exon 3 was sandwiched by *loxP* sequences. When the germline heterozygotes were crossed with mice expressing Cre recombinase in the intestines, the serines and threonine encoded by exon 3 and to be phosphorylated by glycogen synthase kinase 3β (GSK3β) were deleted in the offspring intestines, which caused adenomatous intestinal polyps resembling those in $Apc^{\Delta 716}$ knockout mice. Some nascent microadenomas were also found in the colon. These results present experimental genetic evidence that activation of the Wnt signaling pathway can cause intestinal and colonic tumors.

Keywords: cell adhesion/cell migration/colon cancer/Tcf-Lef/Wnt signaling

Introduction

β-catenin is one of the key downstream effectors in the Wnt signaling pathway (reviewed by Cadigan and Nusse, 1997). The Wnt pathway has been implicated in two major biological processes of vertebrates: early embryonic development (reviewed by Wodarz and Nusse, 1998) and tumorigenesis (reviewed by Polakis, 1999). The initial clue for the Wnt signaling involved in tumorigenesis was the discovery of *Wnt1* (originally termed *int1*) as an oncogene that can transform mouse mammary epithelial cells (Nusse and Varmus, 1982). Subsequently, it was found that adenomatous polyposis coli (APC) tumor suppressor protein binds to β-catenin (Rubinfeld *et al*., 1993; Su *et al*., 1993), and that the wild-type APC but not mutant APC downregulates β-catenin (Munemitsu *et al*., 1995). Recently, stabilizing mutations were found in the β-catenin gene in melanoma and colorectal cancer cell lines (Morin *et al*., 1997; Rubinfeld *et al*., 1997), and the list of cancers with such β-catenin mutations is expanding rapidly (de la Coste *et al*., 1998; Miyoshi *et al*., 1998; Voeller *et al*., 1998; Zurawel *et al*., 1998; Garcia-Rostan *et al*., 1999; Ogawa *et al*., 1999). These mutations at the serine or threonine residues near the N-terminus prevent the phosphorylation by the APC–axin/conductin–glycogen synthase kinase 3β (GSK3β) complex, and subsequent downregulation of β-catenin (Morin *et al*., 1997; Rubinfeld *et al*., 1997; Zeng *et al*., 1997; Behrens *et al*., 1998; Hart *et al*., 1998; Sakanaka *et al*., 1998). Interestingly, such mutations are present only in colorectal cancer cells that retain the wild-type APC (Sparks *et al*., 1998). When the *APC* gene is mutated so that degradation of β-catenin through phosphorylation by GSK3β is suppressed (Rubinfeld *et al*., 1996; Yost *et al*., 1996; Aberle *et al*., 1997), unphosphorylated and stabilized β-catenin accumulates and moves into the nucleus where it complexes with Tcf4/Lef transcription factors, which initiate transcription of a new set of genes (Behrens *et al*., 1996; Huber *et al*., 1996). While mutations in the β-catenin or APC genes are found in human cancers, homozygous knockout mutations of either of these genes result in early embryonic lethality at the egg cylinder stages (Haegel *et al*., 1995; Moser *et al*., 1995).

To determine the role of β-catenin in the Wnt signaling pathway regarding intestinal tumorigenesis, we constructed by homologous recombination in mouse ES cells, a novel dominant allele of the β-catenin gene (*Catnb*) in which exon 3, which contained all phosphorylation target serine/threonine residues, was sandwiched by the *loxP* sequences. We then generated germline chimeras, and subsequently crossed their offspring with either of two types of mice that expressed Cre recombinase in the intestinal epithelium. In both types of compound heterozygous offspring, intestinal adenomatous polyps were found at young ages. These results provide direct experimental evidence for the involvement of Wnt signaling in intestinal and colonic tumorigenesis.

Results

Construction of mutant mice expressing stable β-catenin in the intestine

In some colon cancer cell lines, mutations have been reported that affect the serine/threonine residues of β-catenin, i.e. S33, S37, T41 and S45, which are targets of phosphorylation by GSK3β (reviewed by Polakis, 1999). In addition, several colorectal cancer cell lines have been reported to carry interstitial deletions in the β-catenin gene that eliminate the whole exon 3 encoding all these residues (Iwao *et al*., 1998; Sparks *et al*., 1998). Accordingly, we constructed a targeting vector, pCatnb-

lox(ex3), in which exon 3 of the mouse β-catenin gene (*Catnb*) was sandwiched by two *loxP* sequences together with a *neo* selection cassette (Figure 1A, top). In this design, future deletion of exon 3 by Cre recombinase should result in mRNA whose exons 2 and 4 are connected in-frame, producing a mutant β-catenin protein in which 76 amino acid residues would be deleted (Figure 1A, bottom). After electroporation into ES cell line RW4, 10 homologous recombinants were identified by PCR followed by Southern hybridization from 672 G418-resistant candidates (Figure 1B). To ensure that the *loxP*-sandwiched exon 3 could be deleted by Cre, we first transfected the targeted ES cells with a *cre* expression vector (pPGK-cre), isolated transfectant cell lines, and

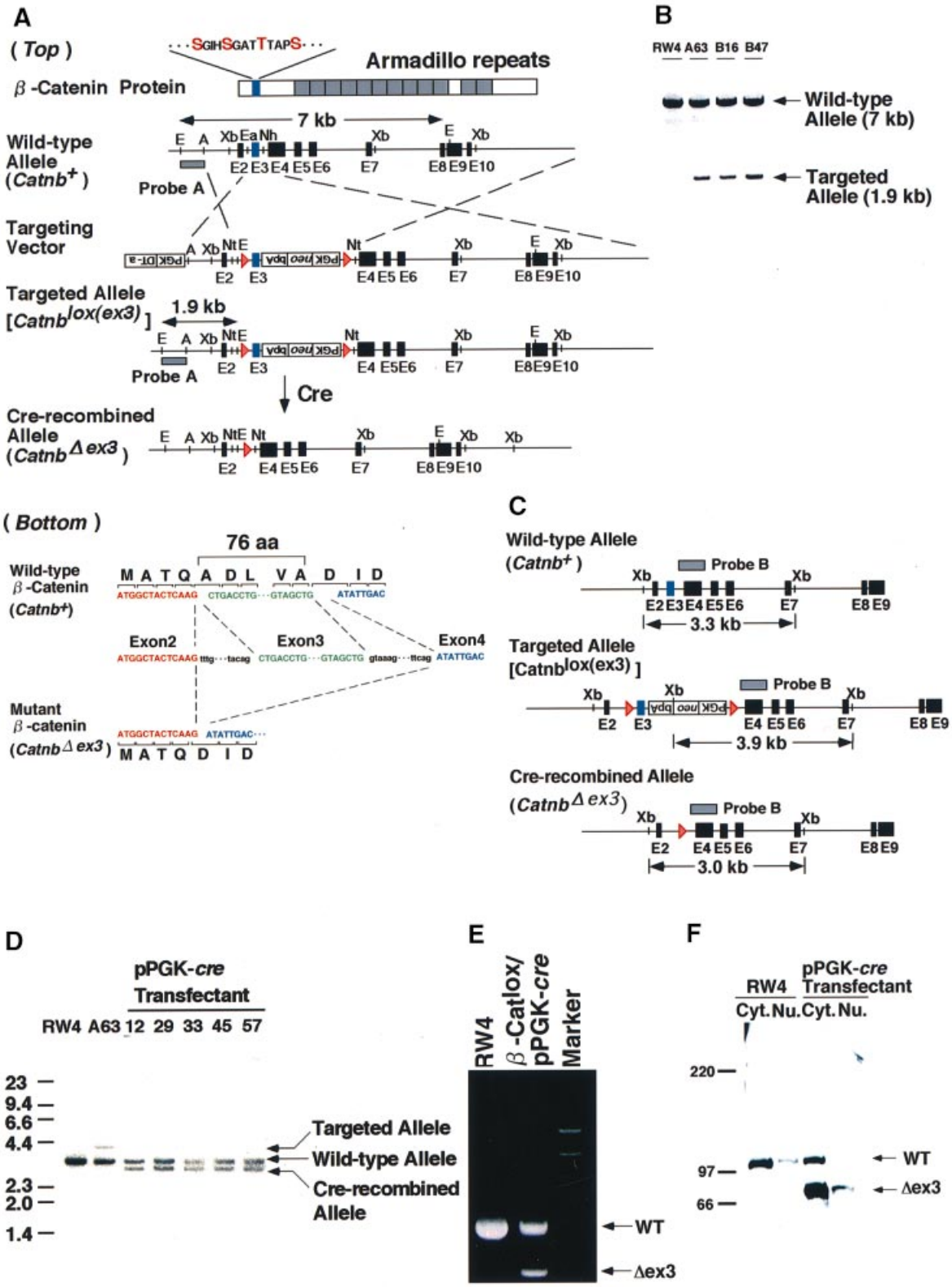

compared their genomic DNA samples with those from the targeted and parental ES cell lines using another Southern hybridization system (Figure 1C). As shown in Figure 1D, the 3.9 kb *Xba*I fragment of the targeted allele [$Catnb^{lox(ex3)}$] was converted to a 3.0 kb band ($Catnb^{\Delta ex3}$) in the transfectant clones, indicating a successful Cre-mediated deletion of exon 3. We further determined the β-catenin mRNA and protein levels in the transfectant ES cells. As seen in Figure 1E, the transfectants showed an RT–PCR band deleted in exon 3, in addition to the wild type. The band for the $Catnb^{\Delta ex3}$ mRNA was weaker than that for the wild type, probably because of the difference in RT–PCR efficiency. In contrast, a Western immunoblot analysis of the transfectant ES cell lysates subfractionated into the cytoplasmic and nuclear fractions showed much more mutated β-catenin protein than the wild type, some of which was distributed in the nucleus (Figure 1F). These results are consistent with the mutational design that should stabilize β-catenin, and gave us a reasonable expectation that exon 3 of the mutant β-catenin allele should be deleted in the mouse tissues where the *cre* gene would be expressed.

We then injected the targeted ES cell clones into C57BL/6N blastocysts, obtained chimeras, and established two germline-transmitted mouse lines [$Catnb^{+/lox(ex3)}$]. On intercrossing, wild-type, heterozygous and homozygous mutant mice were born in the Mendelian ratio (Figure 2A), and both heterozygous and homozygous offspring appeared normal and were fertile. The levels of β-catenin in the intestine and liver analyzed by Western immunoblot analysis were essentially the same in the heterozygous and homozygous mutant mice as in the wild type (data not shown). To introduce the Cre-mediated deletion in the targeted allele [$Catnb^{lox(ex3)}$] of the intestinal epithelium, we constructed two types of Cre-expressing mice. In one type, the *cre* coding sequence was placed under the control of the cytokeratin 19 (Ck19) gene (*Krt1-19*) by a gene knock-in strategy in ES cells ($Krt1\text{-}19^{cre}$; Figure 2B). The Ck19 gene was chosen because it was expressed in the gut epithelium from early stages of embryonic development to adult life (Quaroni *et al*., 1991; data not shown) and it was dispensable (i.e. the homozygous knockout mice were viable, fertile and appeared normal; data not shown). In the other type, a DNA fragment carrying the *cre* coding sequence driven by the enhancer-promoter region (–596 to +21) of the rat liver fatty acid binding protein gene (*Fabpl*) (Simon *et al*., 1993) was injected into fertilized eggs and five independent transgenic mouse lines were established ($Tg{\cdot}Fabpl^{cre}$; Figure 2C).

The targeted mice [$Catnb^{+/lox(ex3)}$ or $Catnb^{lox(ex3)/lox(ex3)}$] were then crossed with either type of Cre-expressing mice. The results of the crosses are summarized in Table I and a genotype analysis of three offspring from such a cross with the Ck19-*cre* mouse strain ($Krt1\text{-}19^{+/cre}$) is shown in Figure 2D. Compound heterozygous mice were obtained with the Ck19-*cre* knock-in mice [$Catnb^{+/lox(ex3)}$:$Krt1\text{-}19^{+/cre}$] as well as with the *Fabpl-cre* transgenic lines [$Catnb^{+/lox(ex3)}$:$Tg{\cdot}Fabpl^{cre}$].

Intestinal polyposis in the stable β-catenin mutant mice

Upon necropsy of the compound heterozygotes with Ck19-*cre* [$Catnb^{+/lox(ex3)}$:$Krt1\text{-}19^{+/cre}$], numerous intestinal polyps in the range of 3000 per mouse were found in all mice at relatively young ages (i.e. by the third week after birth). One of the representative intestinal samples was photographed in Figure 2E, left. Polyps were found at highest densities in the duodenum and proximal jejunum, and at somewhat lower densities in the ileum. A smaller number of polyps were found in the terminal ileum, and essentially none in the cecum or colon, although some nascent microadenomas were found buried in the colonic mucosa (see below). In contrast to the well separated polyps that develop in the $Apc^{\Delta 716}$ knockout mice (Oshima *et al*., 1995), it was difficult to count the polyp numbers precisely in the Ck19-*cre* compound mutants because the polyps were often formed in contiguous sheet-like clusters. We then isolated these polyp clusters and analyzed their DNA by PCR, comparing it with that of the adjacent normal intestinal epithelium, colonic mucosa and liver tissue. As shown in Figure 2G, the deleted β-catenin allele ($Catnb^{\Delta ex3}$) was found only in the polyp adenomas of the duodenum, jejunum and ileum, but not in the adjacent normal mucosa. Interestingly, the deleted allele was also

Fig. 1. Construction of a dominant, stable, β-catenin gene allele by the *cre-lox* system. (**A**) Top, targeting strategy. From top to bottom, the structures are shown for β-catenin protein with the amino acid sequence at the phosphorylation sites (in red), the wild-type allele ($Catnb^{+}$), targeting vector pCatnb-lox(ex3), targeted allele [$Catnb^{lox(ex3)}$] and the Cre-recombined allele ($Catnb^{\Delta ex3}$), respectively. Exons are shown as filled boxes (E1–E10), whereas intronic sequences are shown as solid lines. The PGK-neo-bpA and PGK-DT-a cassettes are shown as open boxes in their transcriptional orientations. Red triangles sandwiching exon 3 (in blue) and PGK-neo-bpA indicate *loxP* sequences. The positions of Southern hybridization probe A and the *Eco*RI (abbreviated as E) fragments to be detected by probe A are also shown [7 and 1.9 kb, respectively; see (B)]. Restriction endonuclease sites are: A, *Apa*I; E, *Eco*RI; Ea, *Ear*I; Nh, *Nhe*I; Nt, *Not*I; and Xb, *Xba*I. Bottom, sequence diagram of the β-catenin deletion mutation. The exon 3 deletion design is shown so that the relationship between the wild-type and the mutant β-catenin can be compared. The genomic DNA sequence is also shown in the middle. The sequences for exons 2, 3 and 4 are shown in red, green and blue, respectively, whereas the intronic sequences are in black and lower case. (**B**) Homologous recombination in the targeted ES cell clones confirmed by Southern hybridization. The *Eco*RI-digested DNA samples were analyzed by hybridization with probe A shown in (A). Lane RW4 was loaded with the DNA from the parental ES cell line RW4, whereas lanes A63, B16 and B47 were loaded with DNAs from the targeted ES clones. (C and D) Cre-mediated recombination in the targeted ES clones transfected with plasmid pPGK-cre confirmed by Southern hybridization. Schematic maps with the *Xba*I (abbreviated as Xb) sites, the probe B (solid bar above exon 4, E4) and the resultant fragments are shown in (**C**), whereas the hybridization phosphoimage is shown in (**D**). The left two lanes were loaded with the DNAs from the parental ES cell line RW4 and the targeted ES clone A63 [$\beta\text{-Cat}^{lox}$, i.e. $Catnb^{+/lox(ex3)}$], respectively, whereas the right five lanes were loaded with DNAs from the pPGK-cre transfectant clones. On the right, band positions for the targeted, wild-type and Cre-recombined alleles are shown (3.9, 3.3 and 3.0 kb, respectively). (**E**) Expression of the mutant β-catenin mRNA in the Cre-mediated recombinant ES cells confirmed by RT–PCR analysis. The left lane was loaded with samples from the parental ES cell line RW4, whereas the middle lane was from the targeted ES cells transfected with the pPGK-cre plasmid ($\beta\text{-Cat}^{lox}$/pPGK-cre). The right lane was loaded with size markers (M; 1.4, 1.1 and 0.9 kb). On the right of the gel, the band positions for the wild-type (WT; $Catnb^{+}$) and mutant (Δex3; $Catnb^{\Delta ex3}$) β-catenin mRNA are shown. (**F**) Expression of the mutant β-catenin protein in the Cre-mediated recombinant ES cells confirmed by Western immunoblot analysis. The cytoplasmic (Cyt.) and nuclear (Nu.) fractions were analyzed using an antibody against β-catenin for the parental ES cell line RW4 and the targeted ES clone (A63) transfected with pPGK-cre. Positions for the wild-type (WT; $Catnb^{+}$) and mutant β-catenin (Δex3; $Catnb^{\Delta ex3}$) are shown on the right. Numbers on the left show positions for the size markers.

detected in the colon (Figure 2G) where no conspicuous polyps were found, but some nascent microadenomas were found buried in the mucosa (see below). Upon Western immunoblot analysis of the polyps as well as the normal mucosa from the compound heterozygotes, the mutant β-catenin protein was expressed only in the intestinal polyps, but not in the normal epithelium adjacent to the polyps (Figure 2H), and the mutant bands were weaker than those for the wild type. This result is in clear contrast to the much stronger mutant band detected in the targeted ES cells transfected with the pPGK-cre expression vector (Figure 1F), and is most likely to be due to the presence of non-epithelial stromal cells in the tumor tissues and/or the Cre-mediated deletion of the *loxP*-sandwiched exon 3 of the β-catenin gene did not take place in all crypt epithelial cells (see Discussion). As anticipated from the genomic DNA analysis (Figure 2G), the band for mutant β-catenin protein was also detected in the colon (Figure 2H). On the other hand, neither the mutant β-catenin allele nor the protein product was detected in

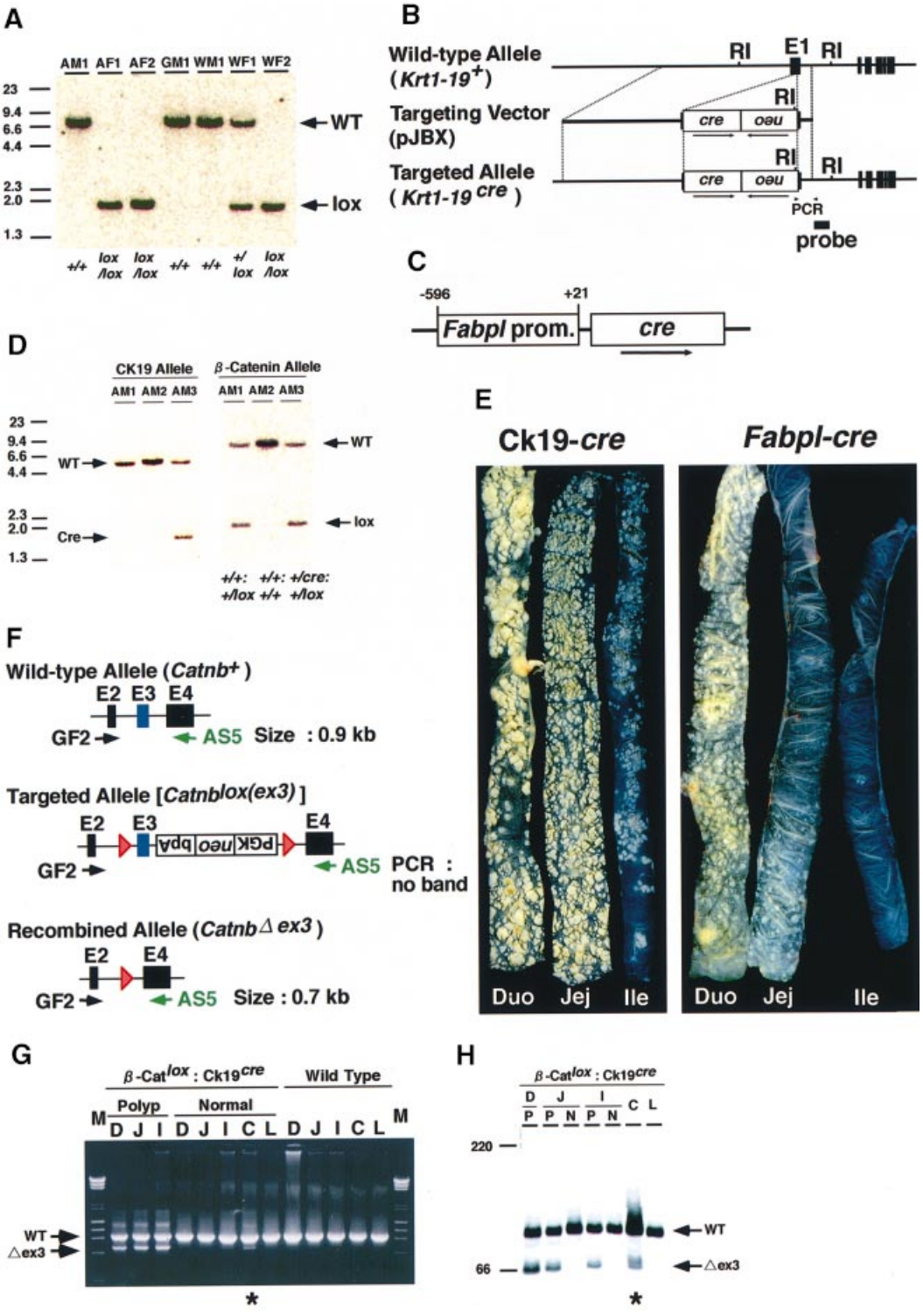

the liver (Figure 2G and H). These compound mutants with Ck19-*cre* survived longer than those with the *Fabpl-cre* transgene (see below) despite their severe polyposis, and died at ~3 months of age due to anemia and cachexia, as $Apc^{\Delta 716}$ heterozygotes do.

In the compound heterozygous mutants carrying the *Fabpl-cre* transgene [$Catnb^{+/lox(ex3)}$:$Tg{\cdot}Fabpl^{cre}$], on the other hand, polyps developed in smaller numbers (~200–700 per mouse) and were more separated from each other (Figures 2E, right, 3A and B). Accordingly, these latter polyps were investigated histologically in more detail. Many polyps were formed by the fourth week after birth (see below), but most mice died within 4–5 weeks from a still unknown cause(s) (Discussion). In 'jelly roll' intestinal samples, polyps were spotted easily as sessile structures (Figure 3C). Upon higher magnifications, the polyp adenomas showed moderate architectural changes of the mucosal epithelium with some budding, branching and resultant crowding patterns that were similar to those in the $Apc^{\Delta 716}$ knockout mice (Figure 3D). It is worth noting that the polyp adenomas were always covered with the normal villus epithelium, as in $Apc^{\Delta 716}$ polyps (M.Oshima *et al*., 1995; H.Oshima *et al*., 1997). Cytologically, rapid cell proliferation was reflected by many mitotic figures and pseudostratified large nuclei (Figure 3F). Upon Alcian blue staining for sulfomucins, no goblet cells or Paneth cells that are stained in the normal intestinal epithelium were found in the polyp adenoma, but it was composed essentially of a single cell type that appeared to be undifferentiated enterocytes (Figure 3E).

To investigate the molecular mechanism of polyp formation, we further analyzed the polyps in the compound heterozygotes [$Catnb^{+/lox(ex3)}$:$Tg{\cdot}Fabpl^{cre}$] by immunohistochemistry. With an anti-β-catenin antibody, prominent staining of the polyp epithelium was found in the nucleus (Figure 4A and B), whereas the basolateral regions were stained in the adjoining normal intestinal epithelium, with a gradient pattern highest at the villus tip and lowest in the crypt bottom (Figure 4C). Interestingly, the extent of nuclear β-catenin staining was heterogeneous even in a small area of a single polyp. This heterogeneity was also observed in the polyps induced by Ck19-*cre* (data not shown) as well as in the $Apc^{\Delta 716}$ polyps (Figure 4D). To rule out possible *Apc* mutations, we then stained the polyp

Table I. Generation of β-catenin mutants by crosses with Cre-expressing mice

Mother	Father	Offspring genotypes (*Catnb*:*cre*[a])			
		+/*lox*:+/*cre*	+/+:+/*cre*	+/*lox*:+/+	+/+:+/+
+/*lox* [$Catnb^{+/lox(ex3)}$]	Ck19-*cre* ($Krt1\text{-}19^{+/cre}$)	7	11	23	19
lox/*lox* [$Catnb^{lox(ex3)/lox(ex3)}$]	Ck19-*cre* ($Krt1\text{-}19^{+/cre}$)	18	0	27	0
+/*lox* [$Catnb^{+/lox(ex3)}$]	*Fabpl-cre1* ($Tg{\cdot}Fabpl^{cre1}$)	9	8	14	7
lox/*lox* [$Catnb^{lox(ex3)/lox(ex3)}$]	*Fabpl-cre1* ($Tg{\cdot}Fabpl^{cre1}$)	9	0	6	0

With another transgenic line *Fabpl-cre5*, only two out of six +/*lox*:+/*cre* mice had small numbers of intestinal polyps. These individuals survived to 13–16 weeks of age, when they were necropsied.
[a]For convenience, the mice without the *Fabpl-cre* transgenes are shown as +/+, whereas mice with one copy of the transgene are shown as +/*cre*.

Fig. 2. Construction of Cre-mediated recombinant β-catenin compound heterozygous mice. (**A**) Southern hybridization analysis of the intercross offsprings of the heterozygotes derived from the targeted ES cell clone carrying the *loxP* allele [$Catnb^{lox(ex3)}$]. Each lane was loaded with *Eco*RI-digested DNA from each mouse, and hybridized with probe A shown in Figure 1A. Genotypes determined are shown on the bottom. (**B**) Construction of mutant cytokeratin 19 (Ck19) gene allele expressing *cre* ($Krt1\text{-}19^{cre}$) by a gene knock-in method in ES cells. From top to bottom, structures of the wild-type allele ($Krt1\text{-}19^{+}$), targeting vector pJBX and the targeted allele ($Krt1\text{-}19^{cre}$) are shown. The *cre* expression cassette (*cre*) and PGK-neo-bpA cassette (*neo*) were inserted into the *Krt1-19* translation initiation site in exon 1 (E1). The arrows indicate their transcriptional orientations. The positions of PCR primers and Southern hybridization probe used for confirmation of homologous recombination are also shown. (**C**) The structure of the DNA fragment used for construction of the *cre*-expressing transgenic mouse lines. The regulatory region of the rat liver fatty acid binding protein gene (*Fabpl* prom.; –596 to +21) was placed upstream of the *cre* coding sequence (see Materials and methods). (**D**) Construction of compound heterozygous mice that carry both the targeted β-catenin [$Catnb^{lox(ex3)}$] and the *cre*-expressing Ck19 alleles ($Krt1\text{-}19^{cre}$). Southern analysis of offspring from a cross between the respective heterozygotes is shown. The DNA samples were digested with *Eco*RI and hybridized with the Ck19 and β-catenin gene probes, respectively. The genotypes determined are shown on the bottom of the right panel. (**E**) Dissection photomicrographs of small intestinal polyps developed in the Cre-mediated recombinant β-catenin mutant mice. Left, a 7-week-old male mouse heterozygous for both β-catenin and Ck19-*cre* alleles [$Catnb^{+/lox(ex3)}$:$Krt1\text{-}19^{+/cre}$]. Right, a 4-week-old female mouse heterozygous for β-catenin and *Fabpl-cre* [$Catnb^{+/lox(ex3)}$:$Tg{\cdot}Fabpl^{cre}$]. The duodenum (Duo), jejunum (Jej) and ileum (Ile) are indicated. (F and G) Cre-mediated deletion of the β-catenin gene exon 3 in the polyp tissues confirmed by PCR analysis. Schematic maps for PCR amplification of the wild-type ($Catnb^{+}$), *loxP*-targeted [$Catnb^{lox(ex3)}$] and Cre-mediated deleted ($Catnb^{\Delta ex3}$) β-catenin alleles with the PCR primers are shown in (**F**), whereas the ethidium-stained gel is shown in (**G**). Note that the PCR for the targeted allele [$Catnb^{lox(ex3)}$] does not result in a visible band under these conditions because of a much longer distance to be amplified. The left three lanes in (G) (Polyp) were loaded with PCR products from the polyp-derived DNAs of the respective tissues, whereas the next five lanes (Normal) were from the normal tissues adjacent to the polyps [β-Cat^{lox}:Ck19*cre*, i.e. $Catnb^{+/lox(ex3)}$:$Krt1\text{-}19^{+/cre}$]. Each lane was loaded with the PCR reaction product amplified on the DNA from the duodenum (D), jejunum (J), ileum (I), colon (C) and liver (L). Note the Δex3 band in the colon of the compound heterozygote (*). Tissues from the wild-type littermates were also analyzed in the right lanes (Wild Type). Band positions for the wild-type (WT) and deleted (Δex3) β-catenin alleles are shown on the left. Lanes M on both ends were loaded with size markers. (**H**) Cre-mediated deletion of the β-catenin exon 3 in the polyp tissues of the compound heterozygotes confirmed by Western immunoblot analysis of the protein product. The total protein from tissues of the polyps (P) or normal mucosa (N) of the duodenum (D), jejunum (J) and ileum (I) as well as from the colon (C) and liver (L) were analyzed as in Figure 1F. Note that the colon (*) showed a band for the mutant β-catenin (Δex3). The positions of the size markers are shown on the left, whereas those for the wild-type (WT) and mutant (Δex3) β-catenin proteins are shown on the right.

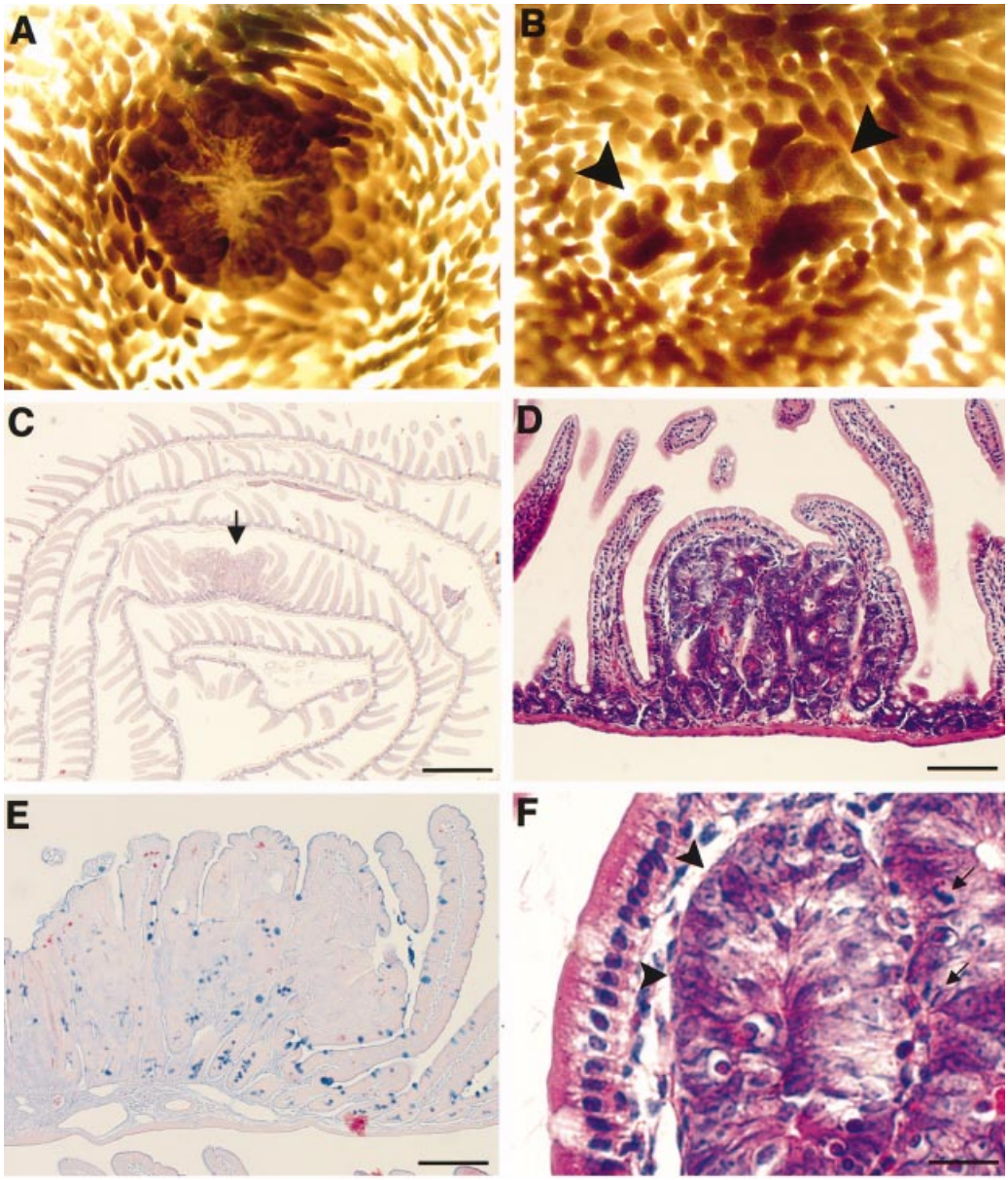

Fig. 3. Morphology of the intestinal polyps developed in the β-catenin mutant mice [*Catnb*$^{+/lox(ex3)}$:*Tg Fabpl*$^{+/cre}$]. (**A**) Dissection micrograph of an intestinal polyp in a 13-week-old *Fabpl-cre5* offspring (male). (**B**) Dissection micrograph of intestinal polyps in a 2-week-old *Fabpl-cre1* offspring (female). Early stage polyps are shown by arrowheads. (C–E) Histological sections of intestinal polyps in the compound heterozygotes. (**C**) A low magnification field of a 'jelly roll' sample. The arrow points to a polyp. (H & E staining). (**D**) A medium magnification field showing a polyp in a mutant mouse of 4 weeks. (**E**) A section of the polyp shown in (A) stained with Alcian blue for sulfomucin. Eosin counterstaining. Note that no blue staining is seen in the polyp adenoma epithelium, whereas the stained cells are goblet cells and Paneth cells in the normal part of the intestinal epithelium. (**F**) A higher magnification of the section in (D) showing the cytological details. Note the mitotic figures (arrows) and nuclear pseudostratification (arrowheads). (H & E staining). Scale bars: (C), 1 mm; (D), 100 μm; (E), 200 μm; (F), 20 μm.

sections with an antibody against the C-terminal region of APC protein. The mutant polyp adenoma epithelium was stained in the same pattern as the normal epithelium (Figure 4E), unlike the polyp adenoma in *Apc*$^{\Delta 716}$ mice which was not stained (Figure 4F). In the proliferating cell nuclear antigen (PCNA) staining for proliferative cells, the polyp epithelial cells in both types of heterozygotes were stained in a similar manner (Figure 4G). Finally, we stained the polyp tissue with an antibody against cyclooxygenase 2 (COX-2). Interestingly, abundant COX-2 expression was found in the stromal cells (Figure 4H) as reported earlier for *Apc*$^{\Delta 716}$ polyps (Oshima *et al*., 1996).

Early polyp morphogenesis in the stable β-catenin mutant mouse

To obtain insights into the polyp initiation mechanism, we investigated early histological patterns in the compound heterozygotes carrying the *Fabpl-cre* transgene [*Catnb*$^{+/lox(ex3)}$:*Tg·Fabpl*^{cre}]. Using a combination of hematoxylin and eosin (H & E) staining and PCNA immunohistochemistry on serial sections of 2- and 4-week-old mouse intestines, we could identify some 'nascent' polyps at the very earliest stages of formation. All nascent polyp adenomas were formed inside the normal villus epithelium, emerging near crypts. Compared with the *Apc*$^{\Delta 716}$ nascent polyps, the adenoma architecture in the β-catenin mutants

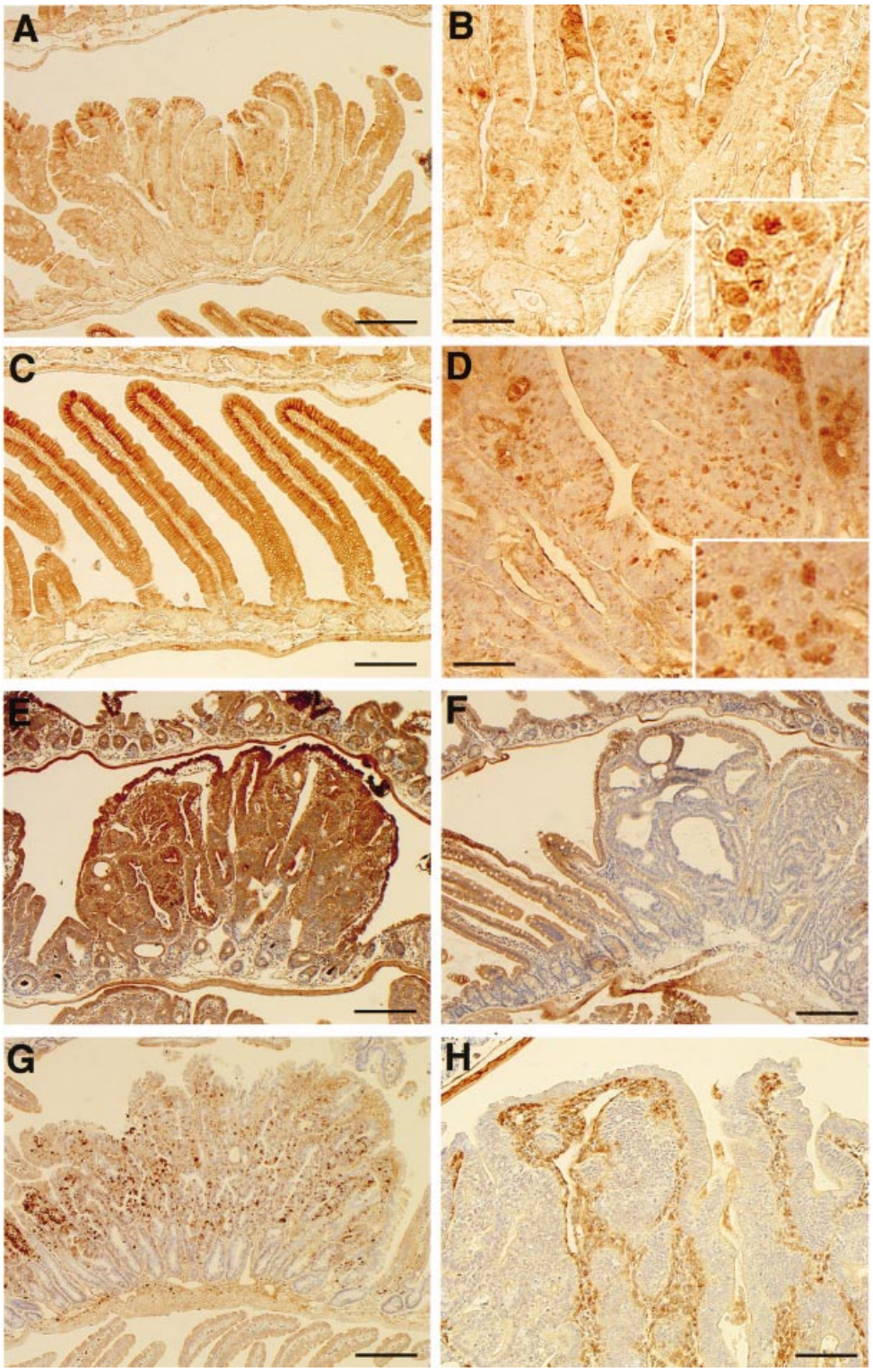

Fig. 4. Molecular characterization of intestinal polyps in the stable β-catenin mutants. (A and B) Immunohistochemical staining for β-catenin of a polyp developed in a 13-week-old compound heterozygote [*Catnb*$^{+/lox(ex3)}$:*Tg·Fabpl*^{cre5}] (male). Low (**A**) and high (**B**) magnification fields, respectively. The inset in (B) shows a sub-field at 3-fold higher magnification. Note the heterogeneous nuclear staining in (B). (**C**) Immunohistochemical staining for β-catenin of the normal intestinal epithelium from the same mouse as in (A) and (B). Note that the staining is essentially in the basolateral regions of the villus epithelium, but not in the crypt. (**D**) Immunohistochemical staining for β-catenin of a polyp developed in a 14-week-old *Apc*$^{\Delta 716}$ mouse (female). The inset shows a sub-field at 3-fold higher magnification. (**E**) Immunohistochemical staining with an antibody against a C-terminal epitope of APC protein of a polyp developed in a 14-week-old compound heterozygote [*Catnb*$^{+/lox(ex3)}$:*Krt1-19*$^{+/cre}$] (male). (**F**) Immunohistochemical staining with an antibody against a C-terminal epitope of APC protein of a polyp developed in a 12-week-old *Apc*$^{\Delta 716}$ mouse (female). (**G**) Immunohistochemical staining for PCNA of a polyp developed in a 13-week-old compound heterozygote [*Catnb*$^{+/lox(ex3)}$:*Tg·Fabpl*^{cre5}] (male). (**H**) Immunohistochemical staining for cyclooxygenase 2 (COX-2) in a 14-week-old compound heterozygote [*Catnb*$^{+/lox(ex3)}$:*Krt1-19*$^{+/cre}$] (male). Magnification bars: (A, E, F and G), 200 μm; (B and D), 50 μm; (C and H), 100 μm.

was more irregular, and heterogeneous in size from the very earliest stages (Figure 5A versus C), which suggests multiple clones initiated concomitantly inside a single polyp. As expected, nuclear staining of β-catenin was evident from these very early stages (Figure 5D).

In addition to the nascent polyp adenomas near the crypt proliferative zone, clusters of cells were found in the adjoining villus epithelium, which showed some signs of dysplasia such as nuclear pseudostratification and positive staining with the PCNA antibody, although little architectural change was observed except slight constrictions of the villus epithelium (Figure 5A and B). Such 'dysplastic cells' have never been observed in *Apc*$^{\Delta 716}$ polyp adenomas. However, these cells did not show nuclear staining with the β-catenin antibody, although the strong staining in the basolateral regions seen in the normal villus epithelium was lost (Figure 5D). The pathological significance of such 'dysplastic cells' remains to be determined.

Although no conspicuous polyps were found in the colon of the compound heterozygotes of either type, ~25 nascent microadenomas per mouse were found under a dissecting microscope in the colon of the mice carrying Ck19-*cre* [*Catnb*$^{+/lox(ex3)}$:*Krt1-19*$^{+/cre}$] (Figure 5E). As shown in the histological sections in Figure 5F–H, these microadenomas were buried in the mucosa and showed similar architectural and cytological changes to those in the nascent polyp adenomas found in the small intestines.

Discussion

In our strategy, exon 3 of one of the β-catenin alleles was deleted by recombination catalyzed by Cre, which was controlled by the regulatory region of either the Ck19 or rat liver fatty acid binding protein (L-FABP) gene. Recombination took place efficiently even though it was difficult to determine the levels of Cre protein in the targeted mouse tissues (data not shown). Although both endogenous Ck19 (Quaroni *et al*., 1991) and the *Fabpl* (–596 to +21) transgene (Sweetser *et al*., 1988) are expressed in the intestinal crypt epithelium, the *cre* gene was probably not expressed in all crypt proliferative zone cells of the knock-in or transgenic mice. Several reasons, as detailed below, may explain our observation that only finite numbers of polyps were formed rather than a contiguous sheet of adenomas all over the intestinal mucosa. In another knock-in mouse line (*Krt1-19*$^{+/lacZ}$), in which a bacterial β-galactosidase gene was placed under the control of the same Ck19 promoter, the LacZ staining in the intestine showed numerous white patches where no *lacZ* was expressed (Y.Tamai and M.M.Taketo, unpublished observation). Although the molecular mechanism remains to be determined, such uneven *lacZ* expression was not observed in other knock-in mice with the *Apc* or *Cdx2* gene (Y.Tamai and M.M.Taketo, unpublished observation). Accordingly, it was possible that the uneven expression of *cre* in the Ck19-*cre* compound heterozygotes was partly due to a heterogeneity in the *Krt1-19* enhancer-promoter activity *in vivo*. On the other hand, in the *Fabpl-cre* transgenic mice (*Tg·Fabpl*^{cre}), the copy number varied widely from one transgenic line to another (data not shown), a phenomenon often observed in transgenic mice including *Tg·Fabpl*$^{Catnb\Delta N89}$ (Wong *et al*., 1998; see below). It was also reported that one of two transgenic lines with the same *Fabpl* enhancer-promoter (–596 to +21) showed heritable mosaic patterns of reporter expression in the intestinal epithelium (Simon *et al*., 1993). It is therefore conceivable that such a mosaic pattern of expression was responsible for uneven expression of *cre*, which resulted in limited numbers of intestinal polyps. In fact, deletion of exon 3 in our compound heterozygotes was found only in the intestine with one transgenic line (*Tg·Fabpl*^{cre5}), whereas a variety of organs including brain, heart, stomach, liver and pancreas showed the PCR band for the deleted allele in the compound heterozygotes with another line (*Tg·Fabpl*^{cre1}; data not shown). While the former lived longer than 13 weeks, the latter died within 4–5 weeks. Accordingly, it is possible that early death of the *Fabpl*^{cre1} compound heterozygotes was due to some deleterious effects of the β-catenin mutation in organs other than the intestine.

Recently, a transgenic mouse line was reported in which N-terminally truncated β-catenin gene was expressed under the control of the rat *Fabpl* gene enhancer-promoter (*Tg·Fabpl*$^{Catnb\Delta N89}$; Wong *et al*., 1998). Although the *Fabpl* regulatory region used in their study was identical to that of ours (i.e. –596 to +21), they found no intestinal polyps or tumors. Instead, increased branching of the intestinal villi was observed at a significantly high frequency. The difference between their results and our present report may be explained as follows. In our design, the β-catenin mutation [*Catnb*$^{lox(ex3)}$] was introduced into one of the endogenous alleles by homologous recombination followed by deletion of *Catnb* exon 3 in the intestine. Accordingly, the mutant β-catenin gene was driven by its own enhancer-promoter. On the other hand, Wong *et al*. (1998) used the *Fabpl* enhancer-promoter to drive the mutant β-catenin gene as a transgene. It is possible that the levels of expression were much lower in the intestine than those of the endogenous β-catenin gene (see below). Another transgenic mouse line was reported recently in which an N-terminally truncated β-catenin gene (*Tg·Krt1-14*$^{Catnb\Delta N87}$) was expressed in the basal epidermis from the cytokeratin 14 enhancer-promoter (Gat *et al*., 1998). The transgenic mice developed benign skin tumors such as trichofolliculomas and pilomatrichomas, which are often found in certain human familial polyposis syndromes. Importantly, they estimated the ΔN87 β-catenin level to be several-fold higher than that of endogenous β-catenin, an observation consistent with our results.

In a morphogenetic analysis of intestinal polyps in the *Apc*$^{\Delta 716}$ knockout mice, we demonstrated earlier that the initial event is formation of an outpocketing pouch by the crypt proliferative zone cells, which then extends into the inner side of adjoining villi (Oshima *et al*., 1997). In the present study, we have observed essentially the same type of polyp morphogenesis. In contrast to the *Apc*$^{\Delta 716}$ knockout mice in which outpocket formation is initiated by loss of the remaining wild-type *Apc* allele in a stochastic manner (Oshima *et al*., 1995), the β-catenin mutation (*Catnb*$^{\Delta ex3}$) in the present experiment was introduced by intestinal expression of the Cre recombinase, which was expected to be initiated in a synchronized manner upon activation of the endogenous Ck19 or L-FABP transgene during development. While Ck19 starts to be expressed in the gut epithelium before 10 d.p.c. (Quaroni *et al*.,

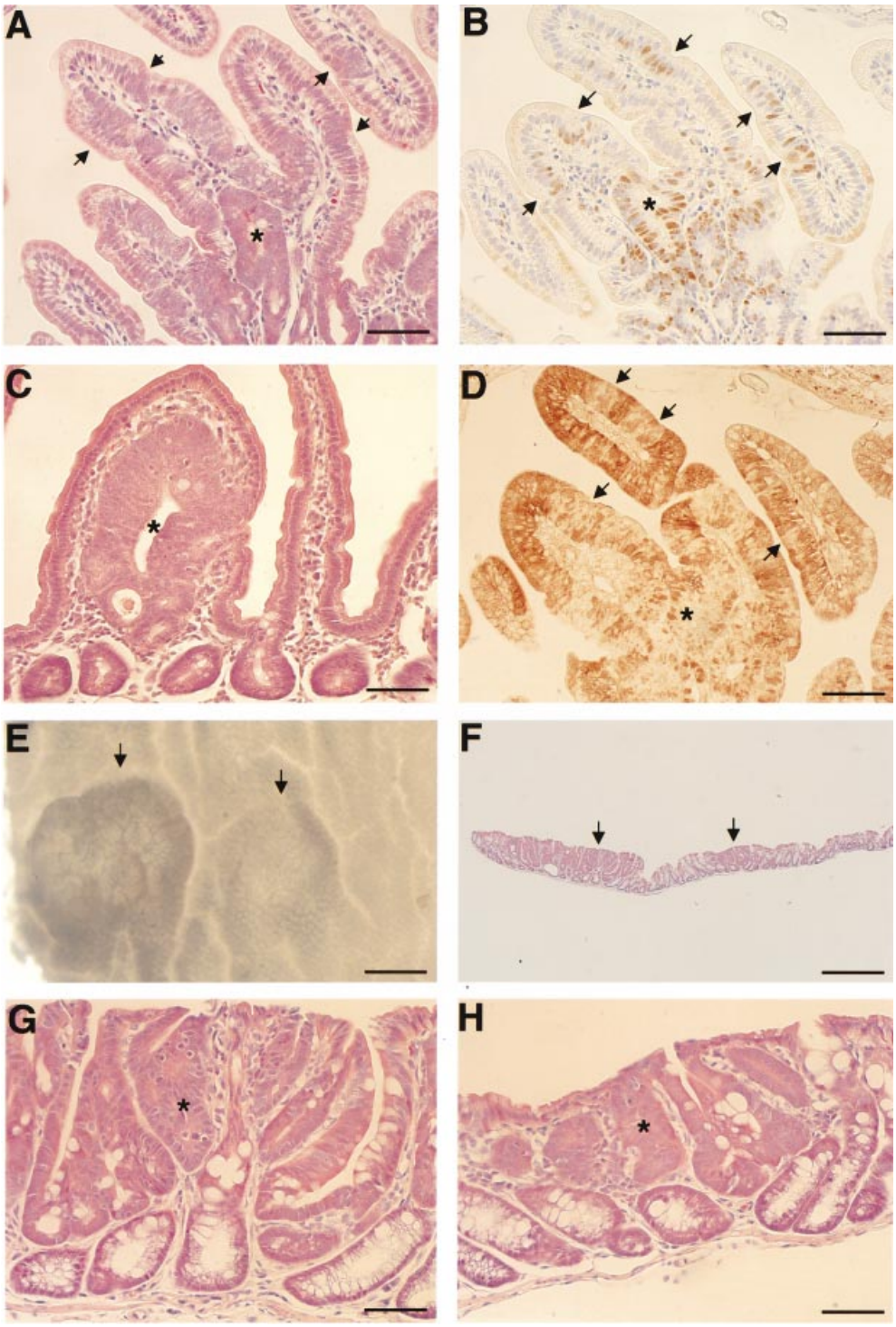

Fig. 5. Nascent polyps in the small intestine (A–D) and colon (E–H). (**A** and **B**) From a 2-week-old female [*Catnb*$^{+/lox(ex3)}$:*Tg·Fabpl*^{cre}] mouse. (A) H & E staining. (B) Immunohistochemical staining for PCNA, with hematoxylin counterstaining. The asterisks indicate a nascent polyp adenoma near crypts, whereas the arrows indicate clusters of 'dysplastic cells' inside the villus region (see the text). Note the constriction of the villi where these clusters exist. (**C**) A nascent polyp (*) developed in a 12-week-old female *Apc*$^{\Delta 716}$ mouse, for comparison. (**D**) Immunohistochemical staining for β-catenin in a nascent polyp of the β-catenin mutant shown in (A) and (B). Note the nuclear staining in the polyp adenoma epithelium (*), and lack of nuclear staining in the 'dysplastic cells' in the villi with altered β-catenin distribution (arrows). Note that (A), (B) and (D) are serial sections. (**E** and **F**) From a 9-week-old female [*Catnb*$^{+/lox(ex3)}$:*Krt1-19*$^{+/cre}$] mouse colon. (E) A dissection micrograph showing two nascent colonic microadenomas (arrows). (F) A low-power view of a histological section of the nascent microadenomas (arrows) shown in (E). (**G** and **H**) High-power views of the histological section through the nascent microadenomas shown in (E) and (F) by arrows. The asterisk in each figure shows one of the microadenoma glands. (A, C, F, G and H), H & E staining. Magnification bars: (A, B, C, D, G and H), 50 μm; (E and F), 500 μm.

1991), a transgene carrying the same *Fabpl* regulatory region as in our *cre* expression construct (i.e. –596 to +21) is expressed in the adult intestinal crypt and colon, but not in the embryonic gut (Sweetser *et al*., 1988). It was therefore anticipated that the exon 3 deletion took place before 10 d.p.c. in the Ck19 compound heterozygotes, but post-natally in the adult of the *Fabpl-cre* offspring. In both types of mutant mice, however, polyps started to form ~2 weeks after birth. It is more likely that this is because the mutated epithelial cell population did not expand until the crypt–villus unit had been established in the second week after birth (Schmidt *et al*., 1988).

It is worth noting that the Cre-recombined allele $Catnb^{\Delta ex3}$ and its protein product were also detected in the colon of the compound heterozygotes [$Catnb^{+/lox(ex3)}$:$Krt1\text{-}19^{+/cre}$] by PCR and Western immunoblot analysis, respectively (Figure 2G and H). Although we could not find any conspicuous polyps in the colon, we did find ~25 nascent microadenomas per mouse buried in the colon of the compound heterozygotes that were 9 weeks old. Such nascent colonic microadenomas were not found in the mice with the $Fabpl^{cre}$ transgene [$Catnb^{+/lox(ex3)}$:$Tg{\cdot}Fabpl^{cre}$] in which deletion of exon 3 was not detected in the colon.

In addition to its role in Wnt signaling, β-catenin plays a key role in cell adhesion as a major component of adherence junctions linking the actin cytoskeleton to members of the cadherin family of transmembrane cell–cell adhesion receptors (Kemler, 1993; Ben-Ze'ev and Geiger, 1998). Moreover, APC and β-catenin are both localized in the adhesion plaques and appear to be involved in cell migration (Näthke *et al*., 1996; Barth *et al*., 1997; Neufeld and White, 1997). On the other hand, mammalian APC binds to tubulin through its C-terminal domain, while such co-localization with tubulin was not observed with *Drosophila* E-APC (Yu and Bienz, 1999). The results we present here, that a stable mutant of β-catenin can still cause intestinal polyps even though it does not appear to affect the interaction with adherence junctions, strongly suggest that polyposis is caused by transcriptional regulation through the Wnt signaling pathway, although direct changes in the interaction with the adherence proteins may also play an additional role.

In conclusion, we constructed mutant mice that carried a dominant and stable β-catenin mutation, which was expressed in the intestinal and colonic epithelia. These mice developed numerous intestinal adenomatous polyps and some colonic microadenomas, demonstrating that activation of the Wnt pathway in the gut can lead to tumorigenesis. These results present direct experimental evidence that Wnt signaling is involved in intestinal tumorigenesis mediated by β-catenin.

Materials and methods

Construction of targeting vectors

β-catenin (Catnb)-loxP targeting construct (Figure 1A). Mouse genomic DNA containing exons 2–10 of the β-catenin gene (*Catnb*, on chromosome 9) were isolated by screening a 129/Sv mouse genomic library in bacteriophage λ (Stratagene, San Diego, CA) using a 1.3 kb mouse cDNA probe (base Nos 98–1362) isolated by RT–PCR. Primers were designed based on the mouse β-catenin sequence (DDBJ/EMBL/GenBank accession No. M90364): BCAT-S1 (5′-ATGGCTACTCAAGCTGACCTGATGG-3′) and BCAT-AS1 (5′-TTACAGGTCAGTATCAAACCAGGCC-3′). PCR was for 30 cycles of 94°C for 30 s, 60°C for 90 s and 72°C for 2 min. A 2.3 kb *Ear*I–*Nhe*I fragment containing exon 3 of *Catnb* and PGK-neo-bpA cassette (Soriano, 1991) was inserted between the two *loxP* sequences in pBS246 (Sauer, 1993). For short and long arms of homology, 1.1 kb *Apa*I–*Bst*XI and 10 kb *Nhe*I–*Mho*I fragments were used, respectively. G418-resistant ES clones were screened by PCR using primers BCAT-F1 (5′-GGTAGTGGTCCCTGCCCTTGACAC-3′) and P85 (5′-CTAAGCTTGGCTGGACGTAAACTC-3′) for 35 cycles of 94°C for 30 s, 60°C for 1 min and 72°C for 1 min. For RT–PCR of the segments shown in Figure 1E, RNA was extracted, reverse-transcribed as above and amplified using the following primers: BCAT-F1 and AS5 (5′-ACGTGTGGCAAGTTCCGCGTCATCC-3′). Homologous recombination in ES cells was verified by Southern hybridization using probe A shown in Figure 1A, as described previously (Oshima *et al*., 1995).

For Western blotting analyses, pPGK-cre-transfected ES cells were lysed in buffer A [10 mM HEPES pH 7.8, 10 mM KCl, 0.1 mM EDTA, 0.1% NP-40]. Cytosolic and nuclear/membrane fractions were separated by centrifugation at 2000 *g* for 1 min at 4°C. Each fraction from 2×10^4 cells was loaded onto a 7.5% SDS–PAGE gel, blotted and detected by a rabbit polyclonal anti-β-catenin antibody (Sigma, MO) coupled with the ECL detection system (Amersham Pharmacia Biotech, Buckinghamshire, UK).

PGK-cre plasmid. From the PGK-neo-bpA cassette (Soriano *et al*., 1991), the *neo* coding sequence between the *Pst*I and *Not*I sites was replaced with the *cre* coding fragment from pBS39 (Sauer, 1987) with adaptors.

Cytokeratin 19 (Ck19)-cre knock-in construct (Figure 2B). A recombinant λ clone was obtained from M.Nozaki, which contained a cytokeratin 19 (*Krt1-19*, on chromosome 11) genomic sequence isolated from a 129/Sv genomic DNA library with a 1.4 kb full-length Ck19 cDNA probe (Ichinose *et al*., 1989). A 6.5 kb *Sal*I–*Kpn*I fragment containing a part of exon 1 and a 641 bp *Kpn*I–*Bgl*II fragment downstream were subcloned for the long and short homology arms, respectively. The ATG translation initiation codon in exon 1 was converted to a *Kpn*I site, and a 365 bp *Kpn*I fragment in exon 1 was replaced with a cassette containing the *cre* coding sequence of pBS39 (Sauer, 1987) and the polyadenylation signal sequence from pPGKneobpA (Soriano *et al*., 1991). Thus, the targeting vector pJBX-cre carried a long homology arm of 6.1 kb (Figure 4B) and was linearized at the unique *Sse*8387I site. Clones resistant to G418 (Geneticin, Sigma) were screened for recombinants by PCR using the following primers, amplifying a fragment of 739 bp: PGKra (5′-CTAAAGCGCATGCTCCAGACT-3′) and Ck19-R2G (5′-CCTGACTAGATTCAAGTTAACTG-3′). Candidates for homologous recombinants were confirmed by Southern hybridization using two probes: a 630 bp *Pst*I–*Xba*I fragment containing the PGK-neo-bpA sequence (not shown); and a 556 bp fragment, located downstream of the vector sequence (Figure 2B). The wild-type *Krt1-19* allele was identified by PCR using primers Ck19-R2G (above) and Ck19-25 (5′-TGGCGGAGTCCGCGGTGGAAGTT-3′), amplifying a fragment of 958 bp. Amplification was for 35 cycles; 1 min at 94°C, 2 min at 60°C and 2 min at 72°C.

L-FABP (Fabpl)-cre transgenic construct (Figure 2C). The enhancer-promoter fragment (–596 to +21) of the L-FABP gene (*Fabpl*, on chromosome 6; Simon *et al*., 1993) was amplified from a rat genomic DNA by PCR using primers that carried *Xho*I and *Sal*I sequences outside of –596 and +21, respectively, and cloned into the respective sites of the pT7BlueT vector (Novagen). In *cre*-carrying plasmid pBS39 (Sauer, 1987), the translation initiation signal was altered to give optimal translation (Kozak, 1987). The *Fabpl* (–596 to +21) fragment and the *cre* sequence above were cloned into pBluescriptII SK^- (Stratagene). From the resulting plasmid, the whole-insert fragment was excised by *Xho*I–*Sca*I digestion, and injected into [C57BL/6×SJL] F_2 fertilized eggs at DNX. Offspring mice were genotyped by PCR of the tail DNA samples using primers CreA (5′-CACGTTCACCGGCATCAACG-3′) and FABP7 (5′-GGTATTTTTCTCCACGTAAT-3′), amplifying a 908 bp fragment. Amplification was for 35 cycles; 30 s at 94°C, 1 min at 55°C and 1 min at 72°C. Five independent transgenic mouse lines were constructed and we analyzed two of them in detail after backcrossing with the C57BL/6N strain for more than three generations.

Generation of knockout mice

ES cell lines D3a2 (Shull *et al*., 1992) and RW4 were obtained from T.Doetschman and Genome Systems (St Louis, MO), respectively. They were cultured and electroporated, and homologous recombinants were

isolated as described (Oshima *et al*., 1995). The Ck19-*cre* mice thus constructed have been backcrossed with the C57BL/6N strain for more than two generations.

Histology and immunohistochemical analyses

Samples were fixed, sectioned and stained with H & E as described previously (Oshima *et al*., 1996). Staining with Alcian blue was performed as described (Takaku *et al*., 1998). A rabbit polyclonal antibody against the C-terminus of human β-catenin, but identical to the corresponding mouse sequence, was obtained from Sigma. Rabbit polyclonal antibodies against human PCNA that cross-react with mouse PCNA, and against the C-terminus of human APC, cross-reacting with mouse APC, respectively, were purchased from Santa Cruz Biotechnology (Santa Cruz, CA). Goat antibody against the C-terminus of rat COX-2, cross-reacting with mouse COX-2, was also purchased from Santa Cruz Biotechnology.

Acknowledgements

We thank T.Doetschman for providing the ES cell line, P.Soriano and M.Nozaki for the plasmid constructs, and N.Sugimoto, R.Nakajima and H.Oshima for excellent technical assistance. This work was supported in part by the Joint Research Fund between the University of Tokyo and Banyu Pharmaceutical Co., and grants from Monbusho (MESSC), Japan.

References

Aberle,H., Bauer,A., Stappert,J., Kispert,A. and Kemler,R. (1997) β-catenin is a target for the ubiquitin-proteasome pathway. *EMBO J.*, **16**, 3797–3804.

Barth,A.I.M., Pollack,A.L., Altschuler,Y., Mostov,K.E. and Nelson,W.J. (1997) NH_2-terminal deletion of β-catenin results in stable colocalization of mutant β-catenin with adenomatous polyposis coli protein and altered MDCK cell adhesion. *J. Cell Biol.*, **136**, 693–706.

Behrens,J., von Kries,J.P., Kühl,M., Bruhn,L., Wedlich,D., Grosschedl,R. and Birchmeier,W. (1996) Functional interaction of β-catenin with the transcription factor LEF-1. *Nature*, **382**, 638–642.

Behrens,J., Jerchow,B.-A., Würtele,M., Grimm,J., Asbrand,C., Wirtz,R., Kühl,M., Wedlich,D. and Birchmeier,W. (1998) Functional interaction of an axin homolog, conductin, with β-catenin, APC and GSK3β. *Science*, **280**, 596–599.

Ben-Ze'ev,A. and Geiger,B. (1998) Differential molecular interactions of β-catenin and plakoglobin in adhesion, signaling and cancer. *Curr. Opin. Cell Biol.*, **10**, 629–639.

Cadigan,K.M. and Nusse,R. (1997) Wnt signaling: a common theme in animal development. *Genes Dev.*, **11**, 3286–3305.

de la Coste,A. *et al*. (1998) Somatic mutations of the β-catenin gene are frequent in mouse and human hepatocellular carcinomas. *Proc. Natl Acad. Sci. USA*, **95**, 8847–8851.

Garcia-Rostan,G., Tallini,G., Herrero,A., D'Aquila,T.G., Carcangiu,M.L. and Rimm,D.L. (1999) Frequent mutation and nuclear localization of β-catenin in anaplastic thyroid carcinoma. *Cancer Res.*, **59**, 1811–1815.

Gat,U., DasGupta,R., Degenstein,L. and Fuchs,E. (1998) *De novo* hair follicle morphogenesis and hair tumors in mice expressing a truncated β-catenin in skin. *Cell*, **95**, 605–614.

Haegel,H., Larue,L., Ohsugi,M., Fedorov,L., Herrenkecht,K. and Kemler,R. (1995) Lack of β-catenin affects mouse development at gastrulation. *Development*, **121**, 3529–3537.

Hart,M.H., de los Santos,R., Albert,I.N., Runinfeld,B. and Polakis,P. (1998) Downregulation of β-catenin by human axin and its association with the APC tumor suppressor, β-catenin and GSK3β. *Curr. Biol.*, **8**, 573–581.

Huber,O., Korn,R., McLaughlin,J., Ohsugi,M., Herrmann,B.G. and Kemler,R. (1996) Nuclear localization of β-catenin by interaction with transcription factor LEF-1. *Mech. Dev.*, **59**, 3–10.

Ichinose,Y., Hashido,K., Miyamoto,H., Nagata,T., Nozaki,M., Morita,T. and Matsushiro,A. (1989) Molecular cloning and characterization of cDNA encoding mouse cytokeratin No. 19. *Gene*, **80**, 315–323.

Iwao,K., Nakamori,S., Kameyama,M., Imalka,S., Kinoshita,M., Fukui,T., Ishiguro,S., Nakamura,Y. and Miyoshi,Y. (1998) Activation of the β-catenin gene by interstitial deletions involving exon 3 in primary colorectal carcinomas without adenomatous polyposis coli mutations. *Cancer Res.*, **58**, 1021–1026.

Kemler,R. (1993) From cadherins to catenins: cytoplasmic protein interactions and regulation of cell adhesion. *Trends Genet.*, **9**, 317–321.

Kozak,M. (1987) An analysis of 5′-noncoding sequences from 699 vertebrate messenger RNAs. *Nucleic Acids Res.*, **15**, 8125–8148.

Miyoshi,Y., Iwao,K., Nagakawa,Y., Aihara,T., Sasaki,Y., Imaoa,S., Murata,M., Shimano,T. and Nakamura,Y. (1998) Activation of the β-catenin gene in primary hepatocellular carcinomas by somatic alterations involving exon 3. *Cancer Res.*, **58**, 2524–2527.

Morin,P.J., Sparks,A.B., Korinek,V., Barker,N., Clevers,H., Vogelstein,B. and Kinzler,K.W. (1997) Activation of β-catenin-Tcf signaling in colon cancer by mutations in β-catenin or APC. *Science*, **275**, 1787–1790.

Moser,A.R., Shoemaker,A.R., Connely,C.S., Clipson,L., Gould,K.A., Luongo,C., Dove,W.F., Siggers,P.H. and Gardner,R. (1995) Homozygosity for the *Min* allele of *Apc* results in disruption of mouse development prior to gastrulation. *Dev. Dyn.*, **203**, 422–433.

Munemitsu,S., Albert,I., Souza,B., Rubinfeld,B. and Polakis,P. (1995) Regulation of intracellular β-catenin levels by the adenomatous polyposis coli (APC) tumor-suppressor protein. *Proc. Natl Acad. Sci. USA*, **92**, 3046–3050.

Näthke,I.S., Adams,C.L., Polakis,P., Sellin,J.H. and Nelson,W.J. (1996) The adenomatous polyposis coli tumor suppressor protein localizes to plasma membrane sites involved in active cell migration. *J. Cell Biol.*, **134**, 165–178.

Neufeld,K.L. and White,R.L. (1997) Nuclear and cytoplasmic localization of the adenomatous polyposis coli protein. *Proc. Natl Acad. Sci. USA*, **94**, 3034–3039.

Nusse,R. and Varmus,H. (1982) Many tumors induced by the mouse mammary tumor virus contain a provirus integrated in the same region of the host genome. *Cell*, **31**, 99–109.

Ogawa,K., Yamada,Y., Kishibe,K., Ishizaki,K. and Tokusashi,Y. (1999) β-catenin mutations are frequent in hepatocellular carcinomas but absent in adenomas induced by diethylnitrosamine in $B6C3F_1$ mice. *Cancer Res.*, **59**, 1830–1833.

Oshima,H., Oshima,M., Kobayashi,M., Tsutsumi,M. and Taketo,M.M. (1997) Morphological and molecular processes of polyp formation in $Apc^{\Delta 716}$ knockout mice. *Cancer Res.*, **57**, 1644–1649.

Oshima,M., Oshima,H., Kitagawa,K., Kobayashi,M., Itakura,C. and Taketo,M. (1995) Loss of *Apc* heterozygosity and abnormal tissue building in nascent intestinal polyps in mice carrying a truncated *Apc* gene. *Proc. Natl Acad. Sci. USA*, **92**, 4482–4486.

Oshima,M., Dinchuck,J.E., Kargman,S.L., Oshima,H., Hancock,B., Kwong,E., Trzaskos,J.M., Evans,J.E. and Taketo,M.M. (1996) Suppression of intestinal polyposis in $Apc^{\Delta 716}$ knockout mice by inhibition of cyclooxygenase 2 (COX-2). *Cell*, **87**, 803–809.

Polakis,P. (1999) The oncogenic activation of β-catenin. *Curr. Opin. Genet. Dev.*, **9**, 15–21.

Quaroni,A., Calnek,D., Quaroni,E. and Chandler,J.S. (1991) Keratin expression in rat intestinal crypt and villus cells. *J. Biol. Chem.*, **266**, 11923–11931.

Rubinfeld,B., Sousa,B., Albert,B., Müller,O., Chamberlain,S.H., Masiarz,F.R., Munemitsu,S. and Polakis,P. (1993) Association of the *APC* gene product with β-catenin. *Science*, **262**, 1731–1734.

Rubinfeld,B., Albert,I., Porfiri,E., Fiol,C., Munemitsu,S. and Polakis,P. (1996) Binding of GSK3β to the APC–β-catenin complex and regulation of complex assembly. *Science*, **272**, 1023–1026.

Rubinfeld,B., Robbins,P., El-Gami,M., Albert,I., Porfiri,E. and Polakis,P. (1997) Stabilization of β-catenin by genetic defects in melanoma cell lines. *Science*, **275**, 1790–1792.

Sakanaka,C., Weiss,J.B. and Williams,L.T. (1998) Bridging of β-catenin and glycogen synthase kinase-3β by axin and inhibition of β-catenin-mediated transcription. *Proc. Natl Acad. Sci. USA*, **95**, 3020–3023.

Sauer,B. (1987) Functional expression of the *cre-lox* site-specific recombination system in the yeast *Saccharomyces cerevisiae*. *Mol. Cell. Biol.*, **7**, 2087–2096.

Sauer,B. (1993) Manipulation of transgenes by site-specific recombination: use of Cre recombinase. *Methods Enzymol.*, **225**, 890–900.

Schmidt,G.H., Winton,D.J. and Ponder,B.A. (1988) Development of the pattern of cell renewal in the crypt-villus unit of chimaeric mouse small intestine. *Development*, **103**, 785–790.

Shull,M.M. *et al*. (1992) Targeted disruption of the mouse transforming growth factor-β1 gene results in multifocal inflammatory disease. *Nature*, **359**, 693–699.

Simon,T.C., Roth,K.A. and Gordon,J.I. (1993) Use of transgenic mice to map *cis*-acting elements in the liver fatty acid-binding protein gene (*Fabpl*) that regulate its cell lineage-specific, differentiation-dependent and spatial patterns of expression in the gut epithelium and in the liver acinus. *J. Biol. Chem.*, **268**, 18345–18358.

Soriano,P., Montgomery,C., Geske,R. and Bradley,A. (1991) Targeted disruption of the c-*src* proto-oncogene leads to osteopetrosis in mice. *Cell*, **64**, 693–702.

Sparks,A.B., Morin,P.J., Vogelstein,B. and Kinzler,K.W. (1998) Mutational analysis of the APC/β-catenin/Tcf pathway in colorectal cancer. *Cancer Res.*, **58**, 1130–1134.

Su,L.K., Vogelstein,B. and Kinzler,K.W. (1993) Association of the APC tumor suppressor protein with catenins. *Science*, **262**, 1734–1737.

Sweetser,D.A., Birkenmeier,E.H., Hoppe,P.C., McKeel,D.W. and Gordon,J.I. (1988) Mechanisms underlying generation of gradients in gene expression within the intestine: an analysis using transgenic mice containing fatty acid binding protein–human growth hormone fusion genes. *Genes Dev.*, **2**, 1318–1332.

Takaku,K., Oshima,M., Miyoshi,H., Matsui,M., Seldin,M.F. and Taketo,M.M. (1998) Intestinal tumorigenesis in compound mutant mice of both *Dpc4* (*Smad4*) and *Apc* genes. *Cell*, **92**, 645–656.

Voeller,H.J., Truica,C.I. and Gelman,E.P. (1998) β-catenin mutations in human prostate cancer. *Cancer Res.*, **58**, 2520–2523.

Wodarz,A. and Nusse,R. (1998) Mechanisms of Wnt signaling in development. *Annu. Rev. Cell Dev. Biol.*, **14**, 59–88.

Wong,M.H., Rubinfeld,B. and Gordon,J.I. (1998) Effects of forced expression of an NH_2-terminal truncated β-catenin on mouse intestinal epithelial homeostasis. *J. Cell Biol.*, **141**, 765–767.

Yost,C., Torres,M., Miller,J.R., Huang,E., Kimelman,D. and Moon,R.T. (1996) The axis-inducing activity, stability and subcellular distribution of β-catenin is regulated in *Xenopus* embryos by glycogen synthase kinase 3. *Genes Dev.*, **10**, 1443–1454.

Yu,X. and Bienz,M. (1999) Ubiquitous expression of a *Drosophila* adenomatous polyposis coli homolog and its localization in cortical actin caps. *Mech. Dev.*, **84**, 69–73.

Zeng,L. *et al*. (1997) The mouse *Fused* locus encodes axin, an inhibitor of the Wnt signaling pathway that regulates embryonic axis formation. *Cell*, **90**, 181–192.

Zurawel,R.H., Chiappa,S.A., Allen,C. and Raffel,C. (1998) Sporadic medulloblastomas contain oncogenic β-catenin mutations. *Cancer Res.*, **58**, 896–899.

Received August 11, 1999; revised September 14, 1999; accepted September 15, 1999

Note added in proof

We have found fatty degeneration of the liver in the compound mutants carrying the *Fabpl-cre1* transgene [$Catnb^{+/lox(ex3)}$;$Tg{\cdot}Fabpl^{cre}$], which appears to be the cause of their death within 4–5 weeks after birth.